Title
Recombinant Osteopontin Stabilizes Smooth Muscle Cell Phenotype via Integrin Receptor/Integrin-Linked Kinase/Rac-1 Pathway After Subarachnoid Hemorrhage in Rats

Journal
Stroke, 47(5)

ISSN
0039-2499

Authors
Wu, Jiang
Zhang, Yang
Yang, Peng
et al.

Publication Date
2016-05-01

DOI
10.1161/strokeaha.115.011552

Peer reviewed

HHS Public Access

Author manuscript

Stroke. Author manuscript; available in PMC 2017 May 01.

Published in final edited form as:

Stroke. 2016 May ; 47(5): 1319–1327. doi:10.1161/STROKEAHA.115.011552.

rOsteopontin Stabilizes Smooth Muscle Cell Phenotype via Integrin Receptor/ILK/Rac-1 Pathway after SAH in Rats

Jiang Wu, MD[*], **Yang Zhang, MD**[*], **Peng Yang, MD**, **Budbazar Enkhjargal, PhD**, **Anatol Manaenko, PhD**, **Jiping Tang, MD, PhD**, **William J. Pearce, PhD**, **Richard Hartman, PhD**, **Andre Obenaus, PhD**, **Gang Chen, MD, PhD**[#], and **John H. Zhang, MD, PhD**[#]

Departments of Neurosurgery (J.W., G.C.), the First Affiliated Hospital of Soochow University, Suzhou, China; and Department of Physiology, Loma Linda University, CA (J.W., Y.Z., P.Y., B.E., A.M., J.T., W.J.P., R.H., A.O., J.H.Z.).

Abstract

Background and Purpose—Recombinant Osteopontin (rOPN) has been reported to be neuroprotective in stroke animal models. The purpose of this study is to investigate a potential role and mechanism of nasal administration of rOPN on preserving the vascular smooth muscle phenotype in early brain injury after SAH.

Methods—One hundred and ninety-two male adult Sprague-Dawley rats were used. The SAH model was induced by endovascular perforation. Integrin-linked kinase (ILK) siRNA was intracerebroventricularly injected 48 hours before SAH. The integrin receptor antagonist GRGDSP, FAK inhibitor Fib-14 and Rac-1 inhibitor NSC23766 were administered 1 hour before SAH induction. rOPN was administered via the intracerebroventricular and nasal route after SAH. SAH grade, neurological scores, brain water content, brain swelling, hematoxylin and eosin staining, India ink angiography, Western blots, and immunofluorescence were used to study the mechanisms of rOPN on the vascular smooth muscle phenotypic transformation.

Results—The marker protein of vascular smooth muscle phenotypic transformation alpha-SMA decreased and SMemb increased significantly at 24 and 72 hours in the cerebral arteries after SAH. rOPN prevented changes of alpha-SMA and SMemb, and significantly alleviated neurobehavioral dysfunction, increased the cross-section area and the lumen diameter of the cerebral arteries, reduced brain water content and brain swelling and improved the wall thickness of cerebral arteries. These effects of rOPN were abolished by GRGDSP, ILK siRNA and NSC23766. Intranasal application of rOPN at 3 hrs after SAH also reduced neurological deficits.

Conclusions—rOPN prevented the vascular smooth muscle phenotypic transformation and improved the neurological outcome, which was possibly mediated by the integrin receptor/ILK/Rac-1 pathway.

[#]Correspondence to John H. Zhang, MD, PhD, Department of Physiology and Pharmacology, Loma Linda University, School of Medicine, 11041 Campus St, Risley Hall, Room 219, Loma Linda, CA 92354, USA, johnzhang3910@.yahoo.com, Tel: 909-558-4723; Fax: 909-558-0119, or Gang Chen, MD, PhD, Department of Neurosurgery, the First Affiliated Hospital of Soochow University, 188 Shizi St., Suzhou, 215006, China, nju_neurosurgery@.163.com. Tel: (86)512-67780165; Fax: (86)512-65238033.

[*]Jiang Wu and Yang Zhang contributed equally.

Disclosure: None

Keywords

Vascular Smooth Muscle Cell; Phenotypic Transformation; Recombinant osteopontin; Subarachnoid hemorrhage

Introduction

It is likely that neuroprotection will not occur without the proper control of blood circulation in the brain after subarachnoid hemorrhage (SAH)[1]. The cerebral vascular neural network which includes vascular smooth muscle cells are involved in the pathophysiology of SAH[2, 3]. A recent study indicated that the phenotypic transformation of the vascular smooth muscle may play an important role in vascular dysfunction associated with strokes[4–9].

The vascular smooth muscle of cerebral arteries typically switch from contractile to synthetic type and functionally from contraction to repair and migration after injury or hemorrhagic stroke[10]. The vascular smooth msucle can be stained and visualized with alpha smooth muscle actin (alpha-SMA) and an accurate marker for synthetic vascular smooth muscle cell is SMemb/nonmuscle MHC isoform[11].

Osteopontin (OPN) is a multifunctional extracellular matrix glycoprotein, and by activating its cell surface integrin receptors, has been implicated in the regulation of smooth muscle cells phenotype[12]. The integrin-linked kinase (ILK) and Rac-1 are also reported to preserve smooth muscle cell phenotype[13, 14]. Recombinant OPN (rOPN) has been demonstrated to be beneficial in various stroke models[15], however, no studies have investigated the effect of rOPN on vascular smooth muscle phenotype that contributes to early brain injury after SAH.

In this study, we hypothesized that nasal administration of rOPN attenuated the vascular smooth muscle phenotypic transformation after SAH via integrin receptor/ILK/Rac-1 pathway (Supplemental Figure I).

Materials and Methods

Animals

One hundred and ninety-two male adult Sprague-Dawley rats (Harlan, Indianapolis, IN) weighing 300 to 350 grams were used in this study. All experimental protocols were approved by the Institutional Animal Care and Use Committee of Loma Linda University.

Experimental Design

The experiment was designed as follows (Supplemental Figure II).

Experiment I—To determine the time course of the vascular smooth muscle phenotypic transformation after SAH, thirty-six rats were randomly assigned into 5 groups: sham (n=6), SAH 6 hours (n=6), SAH 12 hours (n=6), SAH 24 hours (n=6), and SAH 72 hours (n=6). Western blots were used to detect the protein expression of α-SMA and SMemb in the cerebral vessels of each group. Double immunohistochemistry staining of SMemb and von

Willebrand Factor (vWF) were also performed in sham (n=2), 24 hours (n=2) and 72 hours after SAH (n=2).

Experiment II—In the outcome evaluation, thirty rats were randomly divided into 4 groups: sham (n=6), SAH (n=6), SAH + Vehicle[16] (5ul sterile phosphate-buffered saline (PBS)) (n=6), SAH + 0.02ng/uL rOPN[15](0.1ng in 5uL sterile PBS; n=6). Vehicle or rOPN was injected intracerebroventricularly 3 hours after SAH onset. Neurological Scores, hematoxylin and eosin staining were assessed at 24 hours after SAH. Double immunohistochemistry staining of SMemb and vWF were also performed in sham (n=2), SAH (n=2) and SAH + 0.02ng/uL rOPN (n=2).

Experiment III—Forty-eight rats were randomly assigned into 8 groups for mechanism study: sham (n=6), SAH + Vehicle (5ul sterile PBS; n=6), SAH + 0.02ng/uL rOPN (0.1ng in 5ul sterile PBS; n=6), SAH + 0.02ng/ul rOPN (0.1ng in 5ul sterile PBS) + GRGDSP[16](100pmol/1ul; n=6), SAH + 0.02ng/ul rOPN (0.1ng in 5ul sterile PBS) + Fib-14[17](0.2mg /5ul; n=6), SAH+ 0.02ng/ul rOPN (0.1ng in 5ul sterile PBS) + 500 pmol scrambled small interfering RNA (siRNA; in 5ul sterile PBS; n=6), SAH + 0.02ng/ul rOPN (0.1ng in 5ul sterile PBS) + 500 pmol ILK siRNA[18] (in 5ul sterile PBS; n=6), SAH + 0.02ng/ul rOPN (0.1ng in 5ul sterile PBS) + NSC23766[19] (30ug/5ul; n=6). Scrambled siRNA or ILK siRNA was intracerebroventricularly injected 48 hours before SAH. GRGDSP is an RGD-dependent integrin receptor antagonist. Fib-14 is the FAK inhibitor and NSC23766 is the specific Rac-1 inhibitor. All three were administered 1 hour before SAH induction. Neurological Scores were performed 24 hours after SAH. Western blots and Rac1-GTP binding assay of cerebral vessels were conducted 24 hours after SAH in all groups (n=6).

Experiment IV—To propose a clinically translational route for rOPN administration, intranasal administration was performed at different time points (1 hour, 3 hour, and 6 hour) after SAH. Seventy-eight rats were randomly assigned into 5 groups: sham (n=18), SAH + Vehicle (50ul PBS; n=18), SAH + 0.1μg/ul rOPN[17](5 μg in 50ul PBS, 1h; n=12), SAH + 0.1μg/ul rOPN (5 μg in 50 ul PBS, 3h; n=18), SAH + 0.1μg/ul rOPN (5 μg in 50 ul PBS, 6h; n=12). Neurological scores, brain swelling, brain water content and India ink angiography were assessed at 24 hours in all groups.

SAH Model and Experimental Protocol

The endovascular perforation model of SAH was produced in rats as described previously[15]. Briefly, with 3% isoflurane, a sharpened 4-0 monofilament nylon suture was inserted rostrally into the internal carotid artery from the external carotid artery stump and perforated the bifurcation of the anterior and middle cerebral arteries. Sham-operated rats underwent the same procedures, except the suture was withdrawn without puncture.

Intracerebroventricular Drug Administration

Intracerebroventricular drug administration was performed as reported previously[20–21]. A burr hole was drilled into the skull according to the following coordinates relative to bregma: 1.5 mm posterior and 1.0 mm lateral. The needle of a 10μL Hamilton syringe (Microliter

701; Hamilton Company, Reno, NV) was inserted through the burr hole into the left lateral ventricle through the burr hole 4.0 mm below the horizontal plane of bregma. Sterile PBS vehicle or 5ul rOPN (0.1ng in 5ul; EMD Chemicals, La Jolla, CA) were administered 3 hours after SAH induction by a pump at a rate of 0.5 ul /min., respectively. GRGDSP (Sigma-Aldrich, St. Louis, MO; 100pmol in 1uL), Fib-14 (Tocris Bioscience, Ellisville, MI; 0.2 mg in 5 μL PBS) or NSC23766 (Santa Cruz Biotechnology; 30ug/5ul) was administered 1 hour before SAH induction. 500 pmol/5ul ILK siRNA or scrambled siRNA (Life Technologies) was infused at the same rate 48 hours before SAH modeling.

Severity of SAH

The severity of SAH was blindly assessed at each sacrifice as previously described[22]. Animals that received a score < 7 were excluded from the study.

Neurological Outcome Assessment

Neurological impairments were blindly evaluated using an 18-point score system known as the Modified Garcia Scale and another 4-point score system known as the beam balance test[23].

Brain Volume and Cerebral Blood Volume

Brain Volume was performed as previously described[24]. Cerebral Blood Volume was performed as previously described[24]. Parallel samples of the brain and arterial blood were harvested for hemoglobin assay according to an established protocol[25]. Cerebral blood volume was calculated based on measured brain hemoglobin and compared with the measured volume of the entire brain.

Brain Water Content

The brains were removed 24 hours after surgery and separated into left hemisphere, right hemisphere, cerebellum, and brain stem. Each part was weighed immediately after removal (wet weight) and once more after drying for 72 hours in 105°C. The percentage of water content was calculated as (wet weight-dry weight)/wet weight[23].

India Ink Angiography

The lumen diameter was determined by India ink angiography 24 hours after SAH, as previously described[15]. The smallest lumen diameter within each vascular segment of intracranial cerebral arteries (sphenoidal segment of the MCA, precommunicating segment of the ACA, intradural ICA, and BA) were measured by a researcher who was blind to the treatment groups three times using ImageJ software (NIH) and a mean value per segment was determined.

Morphometric Analysis

The brain sections encompassing the basilar artery were stained with hematoxylin and eosin according to the routine protocol[24]. Histological photographs were serially captured with a microscope camera. At the predetermined anatomical locations the cross-sectional areas and thickness of basilar artery were measured using Image J software (NIH).

Western Blot Analysis

Western blot tests were performed as reported previously[26]. The circle of Willis blood vessels and BAs were harvested under a microscope and homogenized. Primary antibodies used were anti-SMemb (Abcam), the anti- alpha-SMA, the anti-ILK, the anti- phospho-FAK, the anti- total-FAK, the anti-β-actin, the anti-tubulin (Santa Cruz Biotechnology).

Immunofluorescence Staining

Immunofluorescence staining was performed on the fixed frozen brain sections as previously described[26]. Sections were incubated overnight at 4°C with the anti-SMemb (Abcam), or the anti- alpha-SMA (Santa Cruz Biotechnology) with the anti-vWF (Millipore, Temecula, CA), followed by appropriate fluorescence dye-conjugated secondary antibodies (Jackson Immunoresearch, West Grove, PA) for 2 hours at room temperature. The sections were visualized with a fluorescence microscope (Olympus OX51, Tokyo, Japan).

Rac-1-GTP binding assay

Rac-1 activation assay was performed using PAK1-PBD color agarose beads according to the manufacturer's protocol (Cell Biolabs). Proteins were fractionated by SDS-PAGE and subjected to Western blot analysis using anti-Rac-1-specific antibody[27].

Statistical Analysis

Neurological scores were expressed as median ± 25th-75th percentiles, and were analyzed using Mann-Whitney U tests or Kruskal-Wallis tests, followed by Steel-Dwass multiple comparisons. Other values were expressed as mean ± standard deviation, analyzed by One-way ANOVA followed by a Tukey multiple comparisons test. $P<0.05$ was considered a statistical difference.

Results

Mortality and SAH severity scores

The total mortality of SAH in the present study was 14.06%, 27 of 192 rats. The mortality was not significantly different among the groups, respectively (data not shown). In addition, there was no significant difference in average SAH grading score among the groups in each experiment (Supplemental Figure III).

Expression profile of the marker proteins of vascular smooth muscle phenotype in cerebral vessels after SAH

We investigated whether the marker proteins of vascular smooth muscle phenotype would respond to early brain injury following SAH. Western blot analysis was performed to determine the protein expression of alpha-SMA and SMemb at 6 hours, 12 hours, 24 hours, and 72 hours after SAH (Figure 1A). Results showed that alpha-SMA level decreased as early as 6 hours after SAH, and had its significant depress at 24 hours. Its level continued to decrease at 72 hours, whereas had no significant difference compared to 24 hours (Figure 1C). Additionally, the expression of SMemb was significantly increased in the cerebral vessels 24 hours (Figure 1B) compared to sham animals.

To further identify the result, immunofluorescence analysis was performed for SMemb expression of the middle cerebral artery (MCA) and the basilar artery (BA). The double immunofluorescence staining revealed that the SMemb immunoreactivity increased on the wall of cerebral vessels at 24 hours and 72 hours after SAH (Figure 1D).

Exogenous rOPN treatment improved the neurological deficits and phenotypic transformation of VSMC 24 hours after SAH

A further experiment was conducted to test whether rOPN attenuate the vascular smooth muscle phenotypic transformation after SAH. As shown in Figure 2B, SAH animals demonstrated severe behavior deficits compared to sham animals. The rOPN group was a significant improvement in neurological functions compared to SAH group.

Consistent with neurological improvement, we performed immunofluorescence analysis (Figure 2A) and HE staining (Figure 2C) for the basilar artery, the SMemb immunoreactivity increased at 24 hours after SAH, and the rOPN can reduce the immunoreactivity of the SMemb. Additionally, the cross-section area of the basilar artery in rOPN group were also significantly increased and the wall thickness were significantly reduced compared to SAH (Figure 2D).

GRGDSP inhibitors abolished rOPN-induced the effect of the vascular smooth muscle phenotype

Then we determined which receptor was involved in the beneficial effects observed by rOPN. The integrin receptor antagonist GRGDSP (100pmol in 1uL) was administered. GRGDSP abolished rOPN induced improvement of neurological scores (Figure 3A). To further evaluate the vascular smooth muscle phenotypic transformation, Western blot for ILK and p-FAK were conducted. The results revealed that rOPN treatment stabilized vascular smooth muscle phenotype by significantly improved the expression of ILK and p-FAK (Figure 3B–D) and GRGDSP reversed the expression of rOPN on ILK and p-FAK.

The Inhibitor of FAK failed to attenuate the effects of rOPN on vascular smooth muscle phenotypic transformation 24 hours after SAH

We determined whether the integrin signaling mediators, FAK and ILK, were able to transduce the integrin-dependent regulation mechanisms. The inhibition of FAK (Fib-14, 0.2 mg dissolved in 5 μl PBS) was administered 1 hour before SAH induction did not significantly improve the neurological defect (Supplement Figure IV A) nor modify the marker proteins of phenotype (Supplement Figure IV B–D).

ILK in vivo knockdown and the inhibitor of Rac-1 abolished the effects on vascular smooth muscle phenotypic transformation by rOPN 24 hours following SAH

A set of siRNAs directed against ILK were mixed and administered and the knockdown efficiency was validated by Western blot analysis. ILK levels were significantly reduced compared with the negative control siRNA groups (Supplement Figure V). ILK in vivo knockdown sufficiently abolished the protective effect of rOPN treatment as shown in Modified Garcia Test (Figure 4A).

To further identify downstream pathways of ILK, the levels of active Rac-1 were determined. rOPN protect the vascular smooth muscle phenotype by upregulating the levels of active Rac-1, ILK siRNA pretreatment reserved the upregulated level of active Rac-1 compared to rOPN group, whereas scrambled siRNA did not show those effects (Figure 4B).

To strengthen the role of Rac-1 in the pathway, the inhibitor of Rac-1 (NSC23766, 30ug dissolved in 5 μl PBS) was administered. NSC23766 and ILK in vivo siRNA administration both decreased the levels of alpha-SMA and increased SMemb compared to rOPN treatment group, while scrambled siRNA didn't show those effects (Figure 4C–D).

Intranasal delivery of rOPN ameliorated neurological deficits and improved the brain swelling, brain edema and lumen diameter 24 hours after SAH

To investigate the clinical translational treatment with rOPN, the nasal administration of rOPN (rOPN dissolved in PBS was administered alternately into the left and right nares. 5 μg of rOPN in a total volume of 50 μl was administered intranasally to each animal.) was performed at three different time points (1 hour, 3 hour, 6 hour) after SAH induction. There was a significant improvement in the neurological score at 1 hour and 3 hour treatment group (Figure 5A–5B).

Brain swelling is represented by wet brain weight, brain volume (size), and cerebral blood volume (hemoglobin content). Both brain wet weight and brain volume were significantly increased 24h following SAH. The SAH group showed increased brain water content 24h after SAH in both hemispheres. rOPN treatment at 1 hour and 3 hour groups significantly reduced brain water content in bilateral cerebral hemispheres, whereas treatment at 6 hour didn't have the effect (Figure 5C). rOPN treatment at 1 hour and 3 hours both attenuated increases in wet brain weight and brain volume (Figure 5D) compared with the SAH group. A marked increase in cerebral blood volume was noted after SAH, cerebral blood volume in rOPN treatment at 1 hour and 3 hour groups were both significantly lower (Figure 5D).

India ink angiography was performed to measure the lumen diameter within each vascular segment of intracranial cerebral arteries. The 3 hour treatment group of rOPN significantly increased the lumen diameter in the left ICA, left MCA, left ACA and BA 24 hours post-SAH compared to the SAH group (Figure 6A–6B).

Discussion

This study demonstrated that as the marker proteins of vascular smooth muscle phenotype, the alpha-SMA decreased and SMemb increased significantly at 24 hours after SAH. rOPN alleviated neurological impairment and the vascular smooth muscle phenotypic transformation associated with an increase of ILK and the activation of Rac-1. An RGD-dependent integrin receptor antagonist GRGDSP reduced rOPN-induced ILK upregulating and Rac-1 activation. Knock down of ILK by siRNA and selective Rac-1 inhibition using NSC23766 abolished rOPN-induced preservation of the vascular smooth muscle phenotypic transformation. The nasal administration of rOPN 3 hours after SAH was also effective for preventing vascular smooth muscle phenotype. Taken together, these findings suggested that the phenotypic transformation of vascular smooth muscle was involved in the early brain

injury in experimental SAH and rOPN prevented the phenotypic transformation of vascular smooth muscle after SAH in rats via the integrin receptor/ILK/Rac-1 pathway.

The vascular neural network, which is an extended classical neurovascular unit, represents a new physiological unit to consider for therapeutic development in stroke[1, 3]. The vascular smooth muscle, as an important part of vascular neural network, might be an alternative therapy for early brain injury after SAH. Previous studies suggested that vascular smooth muscle phenotypic transformation may be caused by local tissue pressure or stretch increases and by blood metabolic products after SAH[10, 28]. Contractile vascular smooth muscle contributed to vascular tone and regulation of blood vessel diameter and blood flow distribution[29]. Vascular smooth muscle phenotypic transformation from contractile to synthetic phenotype may result in decreasing auto regulatory capacity and regional cerebral blood flow to enhance brain swelling and brain edema[28, 29]. One of the mechanisms of the BBB breakdown following SAH is the proteolysis of tight junction proteins by matrix metallo proteinases (MMPs)[30]. A previous study indicated that MMP-9 was expressed in the vascular wall and the co-staining for vascular smooth muscle cells showed that the MMP-9 expression localized to the vascular smooth muscle cells after SAH[8]. The switch of vascular smooth muscle phenotype may not markedly affect the size or function of the large arteries in the previous study[1, 31], but some studies reported that unbalanced contractile/synthetic vascular smooth muscle phenotype affected the size of the cerebral arteries and aggravated brain swelling and brain edema[29,30,32]. It is presumed that due to the limited two or three layers of smooth muscle cells in smaller arteries, vascular smooth muscle phenotype change causes the loss of small arteries vascular tone and affects BBB and autoregualtion. The main observations of this study reports that vascular smooth muscle phenotypic transformation may be involved in the pathophysiology of early brain injury after SAH.

Osteopontin binds with RGD-dependent integrins and certain variant forms of CD44, which activate intracellular signaling pathways and mediate OPN's variable biological functions[33]. Endogenous OPN induction has protective effects following ischemic injuries in the various organs, including the kidneys, heart, lungs and brain[33, 34]. Studies on OPN knockout mice further support the beneficial role of OPN in both adult and neonatal stroke models[35]. OPN knockout mice had greater thalamic neurodegeneration after ischemia[36]. FAK, a cytoplasmic tyrosine kinase, and ILK, a serine/threonine protein kinase, are both key signaling components downstream of integrin engagement by its ligand. Binding of a ligand to the integrin receptors initiate its signaling, which leads to the phosphorylation of FAK and the activation of ILK, thereby modulating downstream signaling[37]. In this study, we investigated the role of the two well-known mediators of integrin pathways, ILK and FAK. rOPN stabilized vascular smooth muscle phenotype via phosphorylation of FAK and the activation of ILK. Inhibiting of the RGD-dependent integrin receptor with GRGDSP, leaded to a reduction of ILK and p-FAK. The inhibition of FAK didn't affect the expression of alpha-SMA and SMemb, whereas knockdown ILK by siRNA exacerbated the outcomes and regulated the expression of alpha-SMA and SMemb. The present results indicated that rOPN regulate the alpha-SMA and SMemb and therefore the phenotype switch pathway through ILK but not FAK. ILK-binding protein interacted with Rac-specific guanine nucleotide exchange factor, a-Pix, activating Rac-1 which has an important role in maintaining endothelial barrier integrity[38]. The observations of this study are consistent with previous

reports that the activation of ILK was linked with the levels of active Rac-1, and Rac-1 inhibitor NSC23766 attenuated the vascular protection of rOPN in this study. These observations suggested that Rac-1 activation is a downstream of ILK and is critical for rOPN to stabilize vascular smooth muscle phenotypes. In addition, Rac-1 could inhibit the vascular smooth muscle phenotypic transformation through upregulating of serum response factor (SRF) dependent gene transcription[14].

Intranasal administration provides a direct route to the brain by endocytosis and transport along olfactory nerves or by extracellular flow through intercellular clefts in the olfactory epithelium to diffuse into the subarachnoid space[39]. It is a safe, efficient, non-invasive and clinically translational route to deliver various neuroprotectants[17, 40]. Our previous studies have demonstrated that nasal administration of 5 μg rOPN 30 minutes after SAH attenuated neuronal apoptosis and the reduction of brain water content in rats[17]. In this study, we gave the rOPN at three different time points after SAH to evaluate the most appropriate time of administration. Our data showed that intranasal administration of rOPN 3 hours after SAH significantly stabilized vascular smooth muscle phenotype. This therapeutic window is feasible for clinical translation for SAH patients.

This study has limitations that it is focused on the vascular smooth muscle phenotypic transformation of large cerebral arteries but is not designed to study small arteries or arterioles. Apparently, more evidences from small arteries and arterioles are needed to verify the role of OPN in smooth muscle phenotype switch. In addition, the time of clearance of rOPN from the CSF circulation and the long term effects of OPN on neurological and neurobehavioral outcomes need to be investigated.

Conclusions

This study demonstrated for the first time that the phenotypic transformation of vascular smooth muscle was involved in the pathophysiology of early brain injury in experimental SAH. Extraneous rOPN protected the phenotypic transformation and improved neurological outcome, mediated possibly by the integrin receptor/ILK/Rac-1 pathway. Nasal administration of rOPN three hours after SAH improved functional outcomes by stabilizing the phenotype of vascular smooth muscle. Our results has potentials to lead to a new target for SAH treatment and clinical translation.

Supplementary Material

Refer to Web version on PubMed Central for supplementary material.

Acknowledgments

Sources of Funding

This research was supported by the National Institutes of Health grants NS081740 and NS084921 to Dr. Zhang and the grant from the National Natural Science Foundation of China (number 81500999).

References

1. Zhang JH. Vascular Neural Network in Subarachnoid Hemorrhage. Transl. Stroke Res. 2014; 5:423–428. [PubMed: 24986148]
2. Zhang JH, Badaut J, Tang J, Obenaus A, Hartman R, Pearce WJ. The vascular neural network-a new paradigm in stroke pathophysiology. Nat Rev Neurol. 2012; 8:711–716. [PubMed: 23070610]
3. Alhadidi Q, Bin Sayeed MS, Shah ZA. Cofilin as a Promising Therapeutic Target for Ischemic and Hemorrhagic Stroke. Transl Stroke Res. 2016; 7:33–41. [PubMed: 26670926]
4. Lee MH, Kwon BJ, Seo HJ, Yoo KE, Kim MS, Koo MA, et al. Resveratrol inhibits phenotype modulation by platelet derived growth factor-bb in rat aortic smooth muscle cells. Oxid Med Cell Longev. 2014; 2014:572430. [PubMed: 24738020]
5. Yoshiyama S, Chen Z, Okagaki T, Kohama K, Nasu-Kawaharada R, Izumi T, et al. Nicotine exposure alters human vascular smooth muscle cell phenotype from a contractile to a synthetic type. Atherosclerosis. 2014; 237:464–470. [PubMed: 25463075]
6. Conway LW, McDonald LW. Structural changes of the intradural arteries following subarachnoid hemorrhage. J Neurosurg. 1972; 37:715–723. [PubMed: 4654701]
7. Ohkuma H, Tsurutani H, Suzuki S. Changes of beta-actin mRNA expression in canine vasospastic basilar artery after experimental subarachnoid hemorrhage. Neurosci Lett. 2001; 311:9–12. [PubMed: 11585555]
8. Maddahi A, Povlsen GK, Edvinsson L. Regulation of enhanced cerebrovascular expression of proinflammatory mediators in experimental subarachnoid hemorrhage via the mitogen-activated protein kinase kinase/extracellular signal-regulated kinase pathway. J Neuroinflammation. 2012; 9:274. [PubMed: 23259581]
9. Hasegawa Y, Suzuki H, Uekawa K, Kawano T, Kim-Mitsuyama S. Characteristics of Cerebrovascular Injury in the Hyperacute Phase After Induced Severe Subarachnoid Hemorrhage. Transl Stroke Res. 2015; 6:458–466. [PubMed: 26358229]
10. Edvinsson LI, Povlsen GK. Vascular plasticity in cerebrovascular disorders. J Cereb Blood Flow Metab. 2011; 31:1554–1571. [PubMed: 21559027]
11. Rensen SS, Doevendans PA, van Eys GJ. Regulation and characteristics of vascular smooth muscle cell phenotypic diversity. Neth Heart J. 2007; 15:100–108. [PubMed: 17612668]
12. Gao H, Steffen MC, Ramos KS. Osteopontin regulates α-smooth muscle actin and calponin in vascular smooth muscle cells. Cell Biol Int. 2012; 36:155–161. [PubMed: 22032345]
13. Shen D, Li J, Lepore JJ, Anderson TJ, Sinha S, Lin AY, et al. Aortic aneurysm generation in mice with targeted deletion of integrin-linked kinase in vascular smooth muscle cells. Circ Res. 2011; 109:616–628. [PubMed: 21778429]
14. Shi F, Long X, Hendershot A, Miano JM, Sottile J. Fibronectin matrix polymerization regulates smooth muscle cell phenotype through a Rac1 dependent mechanism. PLoS One. 2014; 9:e94988. [PubMed: 24752318]
15. Suzuki H, Hasegawa Y, Chen W, Kanamaru K, Zhang JH. Recombinant osteopontin in cerebral vasospasm after subarachnoid hemorrhage. Ann Neurol. 2010; 68:650–660. [PubMed: 21031580]
16. Suzuki H, Hasegawa Y, Kanamaru K, Zhang JH. Mechanisms of osteopontin-induced stabilization of blood-brain barrier disruption after subarachnoid hemorrhage in rats. Stroke. 2010; 41:1783–1790. [PubMed: 20616319]
17. Topkoru BC, Altay O, Duris K, Krafft PR, Yan J, Zhang JH. Nasal administration of recombinant osteopontin attenuates early brain injury after subarachnoid hemorrhage. Stroke. 2013; 44:3189–3194. [PubMed: 24008574]
18. Salahpour A, Medvedev IO, Beaulieu JM, Gainetdinov RR, Caron MG. Local knockdown of genes in the brain using small interfering RNA: a phenotypic comparison with knockout animals. Biol Psychiatry. 2007; 61:65–69. [PubMed: 16712807]
19. Tan AM, Stamboulian S, Chang YW, Zhao P, Hains AB, Waxman SG, et al. Neuropathic pain memory is maintained by Rac1-regulated dendritic spine remodeling after spinal cord injury. J Neurosci. 2008; 28:13173–13183. [PubMed: 19052208]

20. Chen Y, Zhang Y, Tang J, Liu F, Hu Q, Luo C, et al. Norrin protected blood-brain barrier via frizzled-4/β-catenin pathway after subarachnoid hemorrhage in rats. Stroke. 2015; 46:529–536. [PubMed: 25550365]
21. Liu F, Hu Q, Li B, Manaenko A, Chen Y, Tang J, et al. Recombinant milk fat globule-EGF factor-8 reduces oxidative stress via integrin β3/nuclear factor erythroid 2-related factor 2/heme oxygenase pathway in subarachnoid hemorrhage rats. Stroke. 2014; 45:3691–3697. [PubMed: 25342030]
22. Sugawara T, Ayer R, Jadhav V, Zhang JH. A new grading system evaluating bleeding scale in filament perforation subarachnoid hemorrhage rat model. J Neurosci Methods. 2008; 167:327–334. [PubMed: 17870179]
23. Garcia JH, Wagner S, Liu KF, Hu XJ. Neurological deficit and extent of neuronal necrosis attributable to middle cerebral artery occlusion in rats. Statistical validation. Stroke. 1995; 26:627–634. discussion 635. [PubMed: 7709410]
24. Ostrowski RP, Colohan AR, Zhang JH. Mechanisms of hyperbaric oxygen-induced neuroprotection in a rat model of subarachnoid hemorrhage. J Cereb Blood Flow Metab. 2005; 25:554–571. [PubMed: 15703702]
25. Choudhri TF, Hoh BL, Solomon RA, Connolly ES Jr, Pinsky DJ. Use of a spectrophotometric hemoglobin assay to objectively quantify intracerebral hemorrhage in mice. Stroke. 1997; 28:2296–2302. [PubMed: 9368579]
26. He Z, Ostrowski RP, Sun X, Ma Q, Tang J, Zhang JH. Targeting C/EBP homologous protein with siRNA attenuates cerebral vasospasm after experimental subarachnoid hemorrhage. Exp Neurol. 2012; 238:218–224. [PubMed: 22944263]
27. Liao J, Ye Z, Huang G, Xu C, Guo Q, Wang E. Delayed treatment with NSC23766 in streptozotocin-induced diabetic rats ameliorates post-ischemic neuronal apoptosis through suppression of mitochondrial p53 translocation. Neuropharmacology. 2014; 85:508–516. [PubMed: 24953831]
28. Shimamura N, Ohkuma H. Phenotypic transformation of smooth muscle in vasospasm after aneurysmal subarachnoid hemorrhage. Transl Stroke Res. 2014; 5:357–364. [PubMed: 24323729]
29. Ohkuma H, Suzuki S, Ogane K. Phenotypic modulation of smooth muscle cells and vascular remodeling in intraparenchymal small cerebral arteries after canine experimental subarachnoid hemorrhage. Neurosci Lett. 2003; 344:193–196. [PubMed: 12812838]
30. Edvinsson L, Larsen SS, Maddahi A, Nielsen J. Plasticity of cerebrovascular smooth muscle cells after subarachnoid hemorrhage. Transl Stroke Res. 2014; 5:365–376. [PubMed: 24449486]
31. Yamaguchi-Okada M, Nishizawa S, Koide M, Nonaka Y. Biomechanical and phenotypic changes in the vasospastic canine basilar artery after subarachnoid hemorrhage. J Appl Physiol (1985). 2005; 99:2045–2052. [PubMed: 16051708]
32. Song JN, An JY, Hao GS, Li DD, Sun P, Li Y, et al. Role of Akt signaling pathway in delayed cerebral vasospasm after subarachnoid hemorrhage in rats. Acta Neurochir (Wien). 2013; 155:2063–2070. discussion 2069-70. [PubMed: 23873121]
33. Denhardt DT, Noda M, O'Regan AW, Pavlin D, Berman JS. Osteopontin as a means to cope with environmental insults: regulation of inflammation, tissue remodeling, and cell survival. J Clin Invest. 2001; 107:1055–1061. [PubMed: 11342566]
34. Meller R, Stevens SL, Minami M, Cameron JA, King S, Rosenzweig H, et al. Neuroprotection by osteopontin in stroke. J Cereb Blood Flow Metab. 2005; 25:217–225. [PubMed: 15678124]
35. Chen W, Ma Q, Suzuki H, Hartman R, Tang J, Zhang JH. Osteopontin reduced hypoxia-ischemia neonatal brain injury by suppression of apoptosis in a rat pup model. Stroke. 2011; 42:764–769. [PubMed: 21273567]
36. Schroeter M, Zickler P, Denhardt DT, Hartung HP, Jander S. Increased thalamic neurodegeneration following ischaemic cortical stroke in osteopontin-deficient mice. Brain. 2006; 129:1426–1437. [PubMed: 16636021]
37. Skuli N, Monferran S, Delmas C, Favre G, Bonnet J, Toulas C, et al. Alphavbeta3/alphavbeta5 integrins-FAK-RhoB: a novel pathway for hypoxia regulation in glioblastoma. Cancer Res. 2009; 69:3308–3316. [PubMed: 19351861]
38. Spindler V, Schlegel N, Waschke J. Role of GTPases in control of microvascular permeability. Cardiovasc Res. 2010; 87:243–253. [PubMed: 20299335]

39. Thorne RG, Emory CR, Ala TA, Frey WH II. Quantitative analysis of the olfactory pathway for drug delivery to the brain. Brain Res. 1995; 692:278–282. [PubMed: 8548316]

40. Doyle KP, Yang T, Lessov NS, Ciesielski TM, Stevens SL, Simon RP, et al. Nasal administration of osteopontin peptide mimetics confers neuroprotection in stroke. J Cereb Blood Flow Metab. 2008; 28:1235–1248. [PubMed: 18364727]

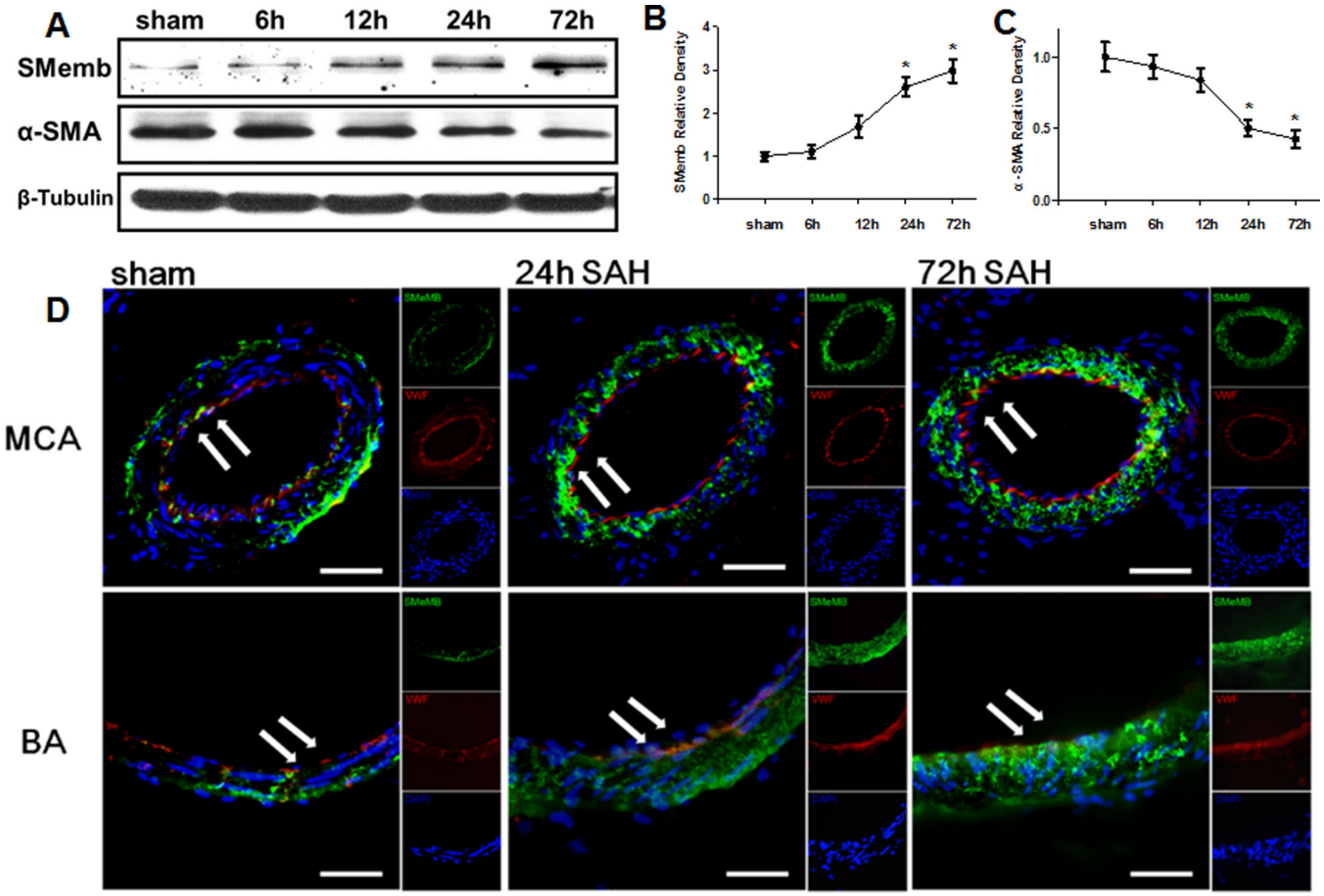

Figure 1.

Expression profile of SMemb and alpha-SMA in cerebral vessels after SAH. **(A)** Expression time curve of SMemb and alpha-SMA in the cerebral vessels within 72h after SAH. **(B) (C)** Quantitative analyses of SMemb and alpha-SMA time course after SAH. **(D)** Immunofluorescence staining for SMemb (green), vascular endothelial cell (VWF) (red), and DAPI (blue) in the walls of middle cerebral artery (MCA) and basilar artery (BA). Scale bars: top panels—50μm; below panels—25um. Relative densities have been normalized against the sham group. n=6 rat per group, per time point. *P<0.05 vs. Sham.

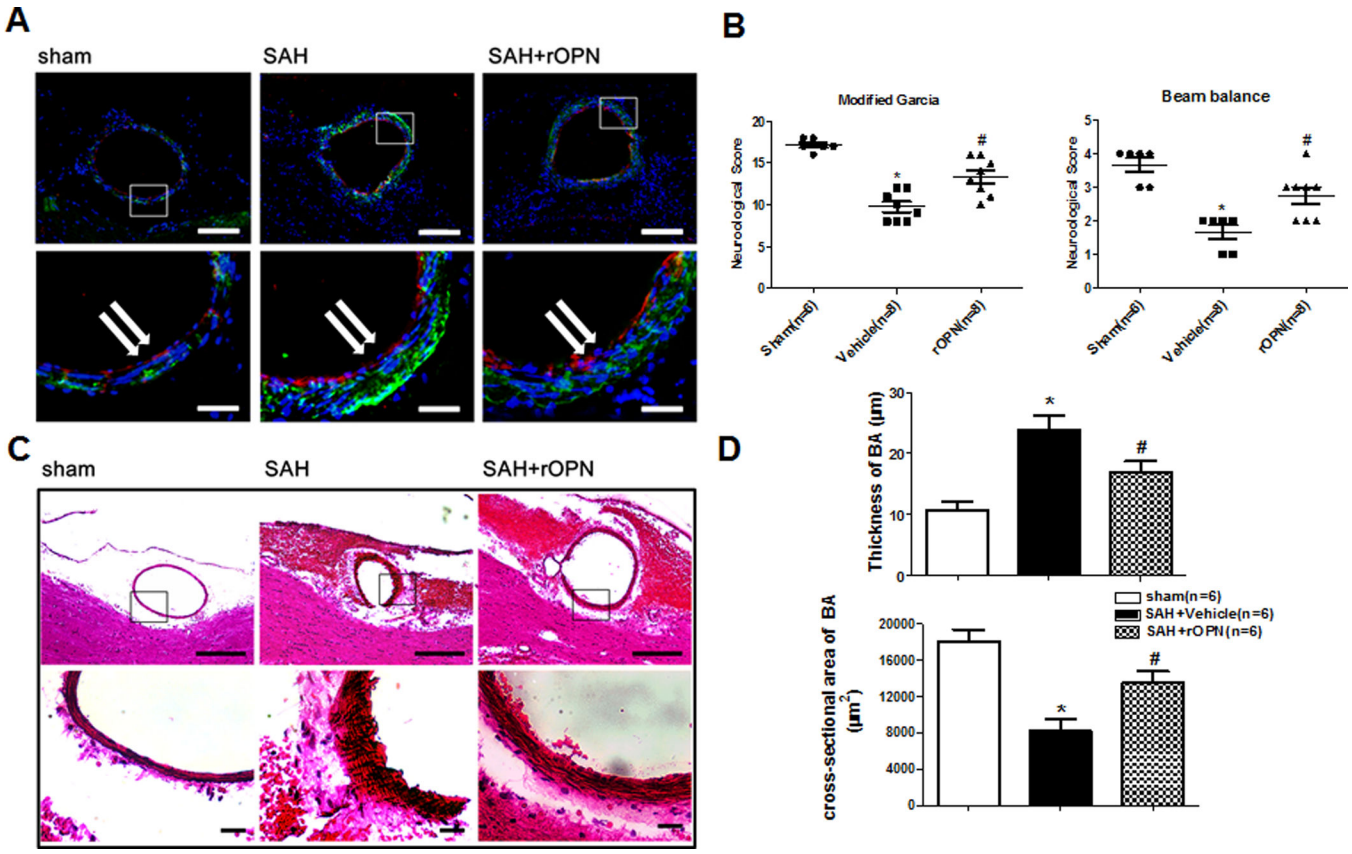

Figure 2.

rOPN treatment improve the marker protein expression of VSMC phenotype, neurological deficits and the cross-section area and wall thickness of the basilar artery 24h after SAH. **(A)** Immunohistochemistry staining for SMemb (green), vascular endothelial cell (red) and DAPI (blue) of the BA transect sections Scale bars: top panels—100um; below panels—25um. **(B)** Modified Garcia test and Beam balance in indicated groups at 24 hours following SAH. **(C)** Representative photographs of HE stain for BA cross sections. Scale bars: top panels—100um; below panels—10um. **(D)** Quantitative analyses of the cross-section area and the wall thickness of BA at 24 hours after SAH. *p < 0.05 vs. sham, #p <0.05 vs. Vehicle.

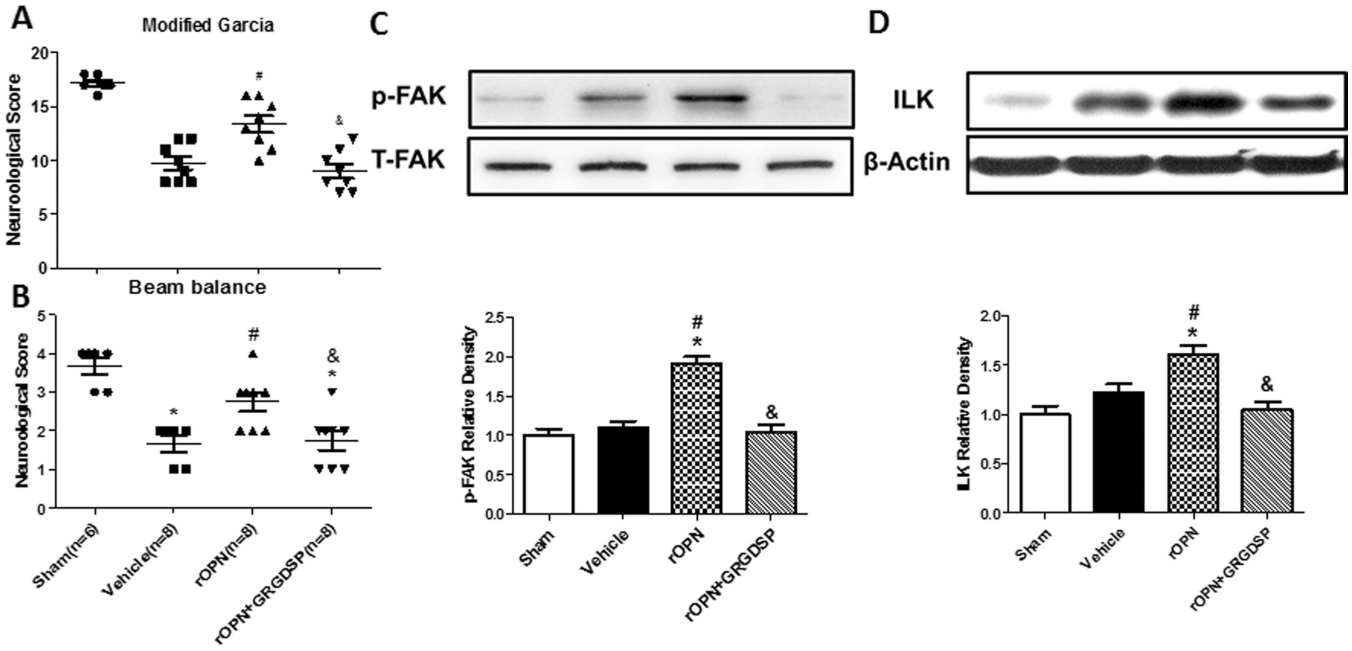

Figure 3.

rOPN prevents VSMC phenotypic transformation by boosting integrin receptors signaling 24h after SAH. Modified Garcia test **(A)** and beam balance **(B)** in indicated groups 24 hours following SAH. Expression change and Quantitative analysis of p-FAK **(C)** and ILK **(D)** in the cerebral vessels 24 hours following SAH. Relative densities have been normalized against the sham group. n=6 rats per group. *P<0.05 vs. Sham; #P<0.05 vs vehicle. &P<0.05 vs rOPN.

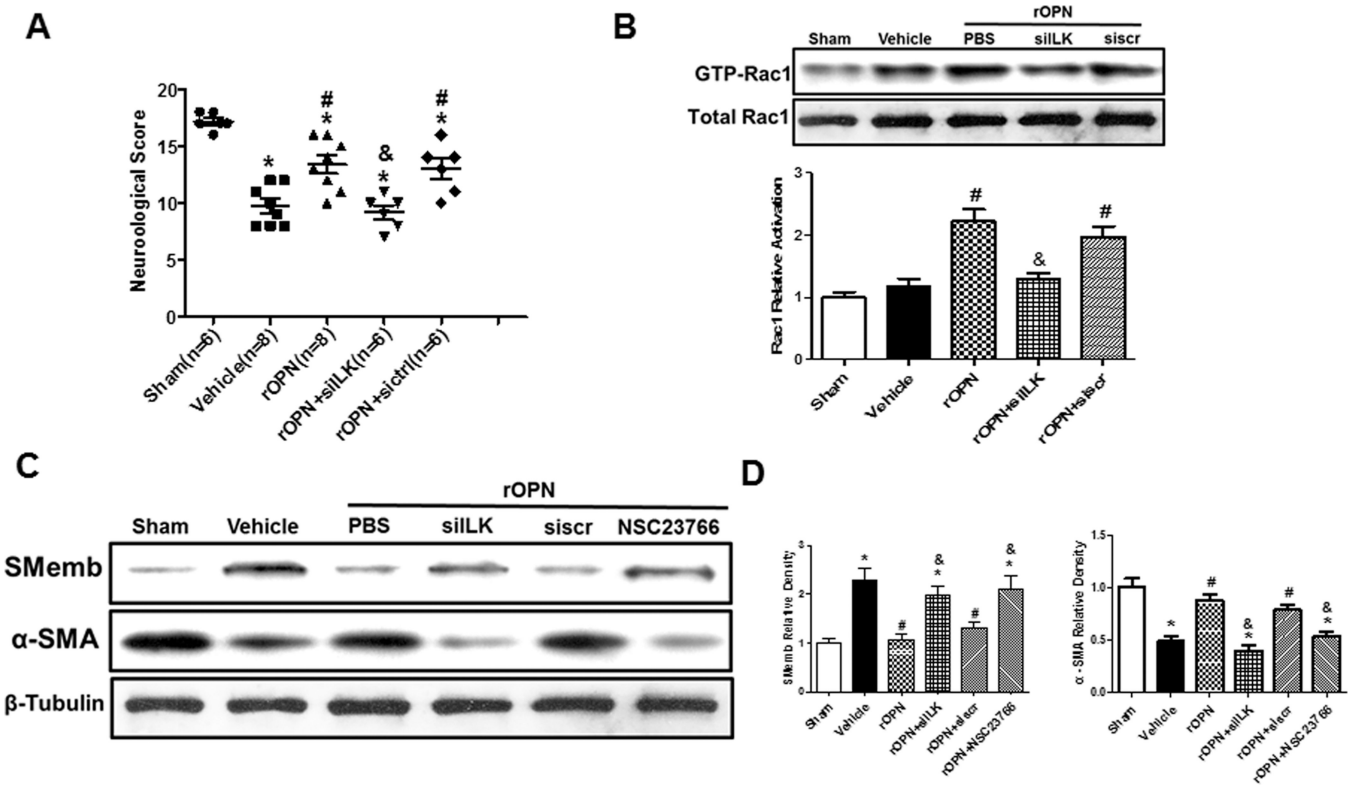

Figure 4.

rOPN attenuated the VSMC phenotypic transformation via integrin receptor / ILK / Rac-1 pathway after SAH. Modified Garcia test in indicated groups at 24 hours following SAH **(A)**. The levels and Quantitative analysis of active Rac-1 were determined in each group **(B)**. Expression change of alpha-SMA, SMemb in the cerebral vessels 24 hours following SAH **(C)**. Quantitative analysis of SMemb and alpha-SMA **(D)**. Relative densities have been normalized against the sham group. n=6 rats per group, *P < 0.05 vs. Sham; #P<0.05 vs vehicle. &P<0.05 vs rOPN.

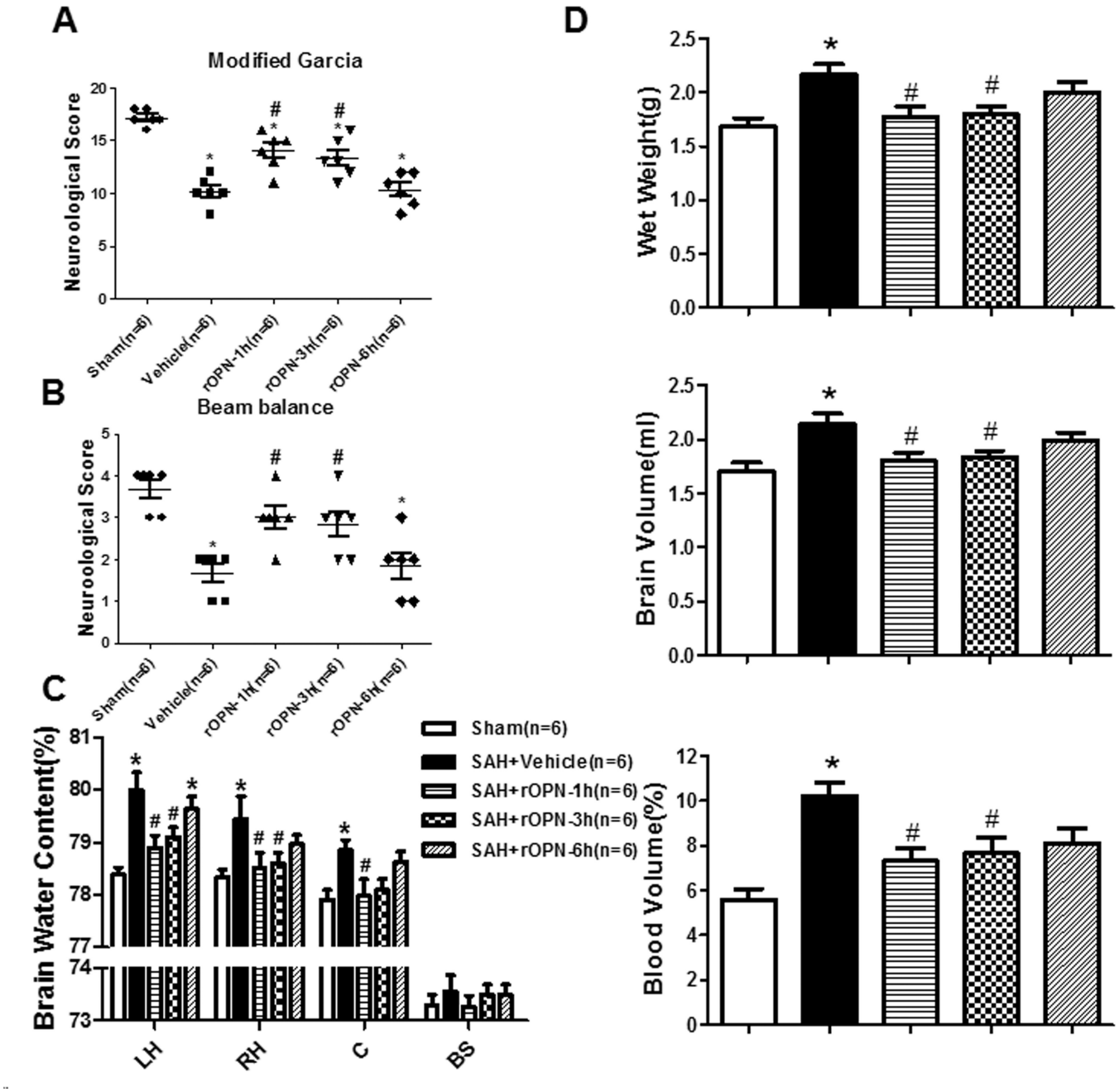

Figure 5.

rOPN by intranasal ameliorated neurological deficits and improved the brain swelling and brain edema 24 hours after SAH. rOPN by intranasal ameliorated neurological deficits of Modified Garcia test **(A)** and beam balance **(B)** in indicated groups 24 hours following SAH. rOPN treatment attenuated brain water content assessment **(C)** and brain swelling **(D)** of Wet brain weight, Blood volume, and brain volume at 24 hours after SAH, n=6 rats per group.*p <0.05 vs. sham, #p <0.05 vs. Vehicle.

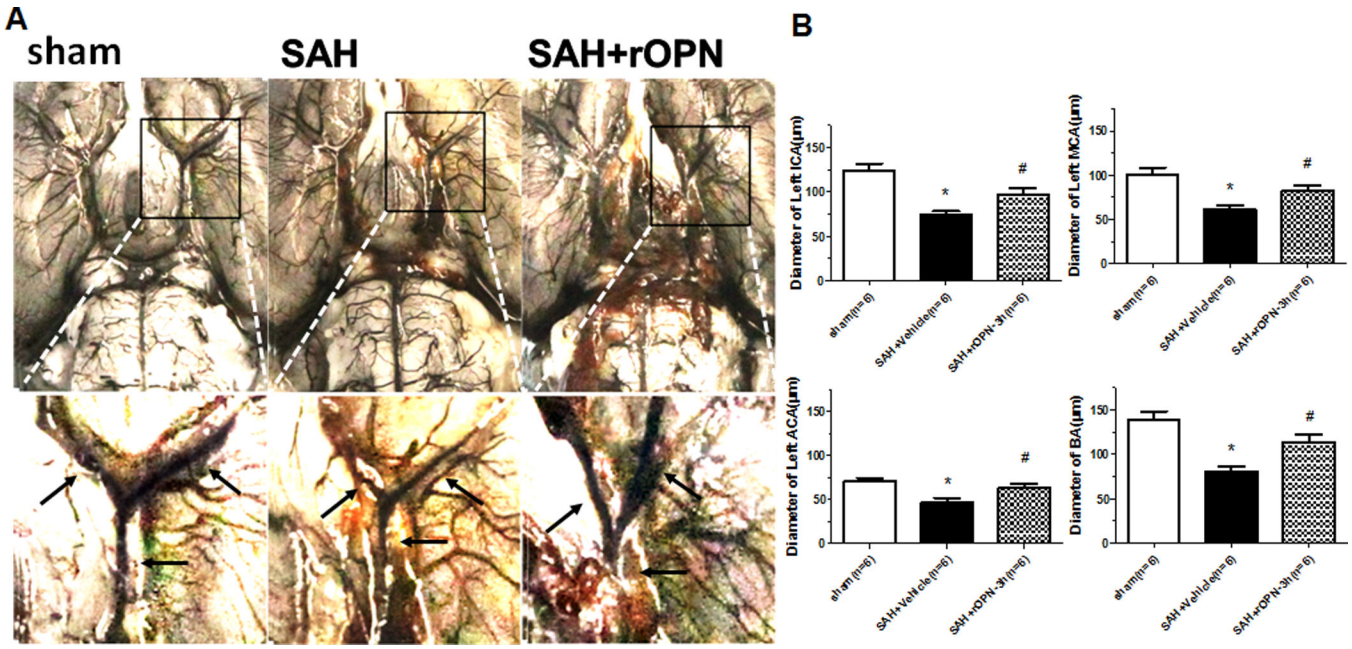

Figure 6.

rOPN by intranasal at 3h after SAH improved the diameter of cerebral artery at 24 hours after SAH. **(A)** Representative India ink angiograms. **(B)** Quantitative analysis of the diameter of ICA, MCA, ACA, BA at 24h after SAH, n=6 rats per group.*p <0.05 vs. sham, #p <0.05 vs. Vehicle.